Science Advances
AAAS

advances.sciencemag.org/cgi/content/full/5/7/eaav1035/DC1

Supplementary Materials for

Nanoparticle-laden droplets of liquid crystals: Interactive morphogenesis and dynamic assembly

Yunfeng Li*, Nancy Khuu, Elisabeth Prince, Moien Alizadehgiashi, Elizabeth Galati, Oleg D. Lavrentovich*, Eugenia Kumacheva*

*Corresponding author. Email: ekumache@chem.utoronto.ca (E.K.); olavrent@kent.edu (O.D.L.); yflichem@jlu.edu.cn (Y.L.)

Published 5 July 2019, *Sci. Adv.* **5**, eaav1035 (2019)
DOI: 10.1126/sciadv.aav1035

This PDF file includes:

Figure S1 shows the TEM images of the CNCs and latex nanoparticles (NPs) that were deposited and dried on the TEM grids.

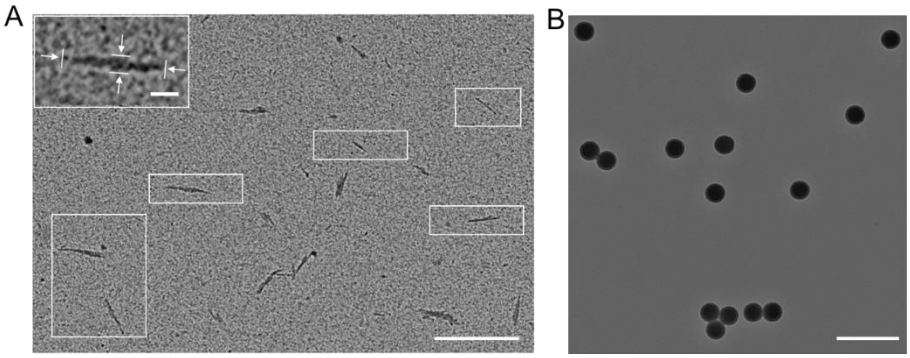

Fig. S1. TEM characterization of CNCs and latex NPs. TEM images of CNCs (**A**) and latex NPs (**B**) that were deposited on a TEM grid from the corresponding aqueous dispersions. The inset in (A) shows the size measurement positions on an individual CNC. The scale bar is 500 nm. In inset the scale bar is 50 nm.

Figure S2 shows the optical microscopy image of the microfluidic device and the NP/Ch-CNC droplets.

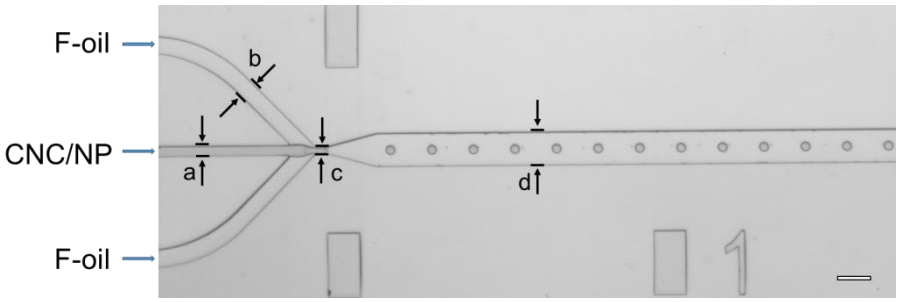

Fig. S2. Optical microscopy images of the Ch-CNC/NP droplets generated in the MF flow-focusing droplet generator. a=30 μm, b=50 μm, c=10 μm, and d=100 μm. The height of the channel was 28 μm. Scale bar is 100 μm. The flow rates of F-oil and Ch-CNC/NPs were 0.2 and 0.02 mL/h, respectively.

Figure S3 shows low magnification images of the NP/Ch-CNC droplets. The latex NPs formed assemblies localized at the two opposite poles of the droplets, in the toroidal rings, in the droplet core and in disclinations in the Ch-CNC shell. These three types assemblies co-existed in different ratios.

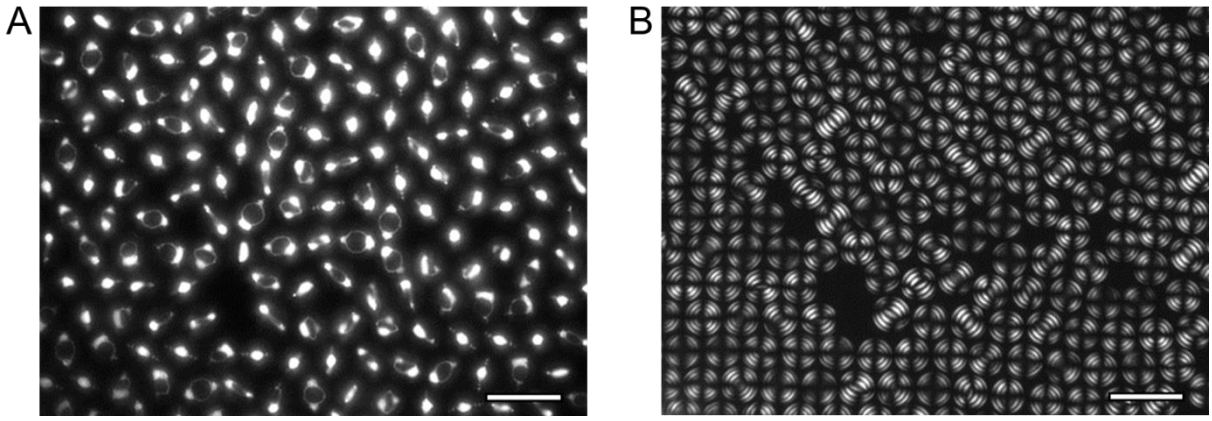

Fig. S3. Characterization of the Ch-CNC droplets loaded with latex NPs. Representative fluorescence microscopy (**A**) and POM (**B**) images of the same Ch-CNC droplets loaded with latex NPs at $\phi_{NP} = 1.1\times10^{-3}$. $\phi_0=4.3\times10^{-2}$ .The scale bars are 50 μm.

Figure S4 shows the POM (A) and fluorescence microscopy images (B) of 100 μm-diameter Ch-CNC droplets (note that the CNCs are autofluorescent). The CNCs were localized in both the isotropic cores and the Ch shells, because the cores had almost the same fluorescence intensity as the Ch-CNC shells (fig. S4B).

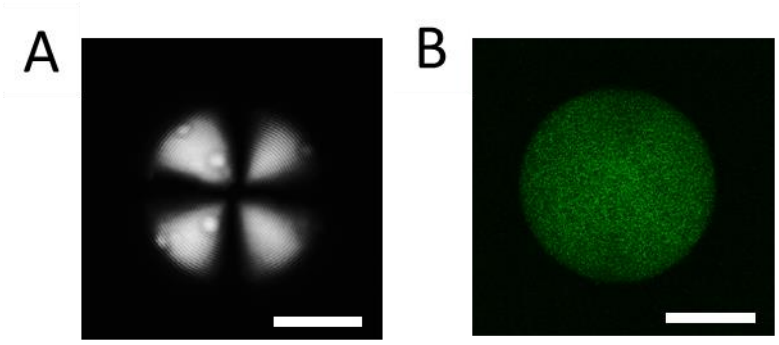

Fig. S4. Characterization of the NP-free Ch-CNC droplets. The POM (**A**) and fluorescence microscopy (**B**) images of 100 μm-diameter Ch-CNC droplets. The scale bar is 50 μm.

Figure S5 shows the photographs of the phase-separated mixtures of the Ch-CNC suspension and latex NPs.

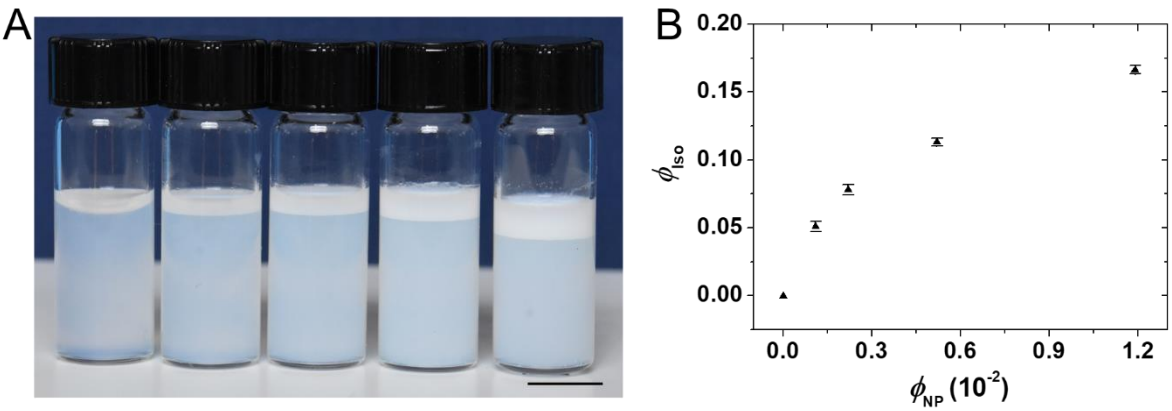

Fig. S5. Phase separation of mixtures of Ch-CNC suspension and latex NPs. (**A**) Photographs of the phase separated mixtures of Ch-CNC suspension and latex NPs. ϕ_0 =4.3×10^{-2}, and ϕ_{NP} (left to right) is 0, 0.11×10^{-2}, 0.22×10^{-2}, 0.52×10^{-2}, and 1.19×10^{-2}. The scale bar is 1 cm. (**B**) Variation in the volume fraction of the isotropic NP-rich phase, plotted as a function of NP volume fraction in the NP/Ch-CNC suspension after 35 day equilibration. (Photo credit: Yunfeng Li, University of Toronto).

Figure S6 shows the schematic of the flat-ellipsoidal droplet structure of the Ch-CNC droplets.

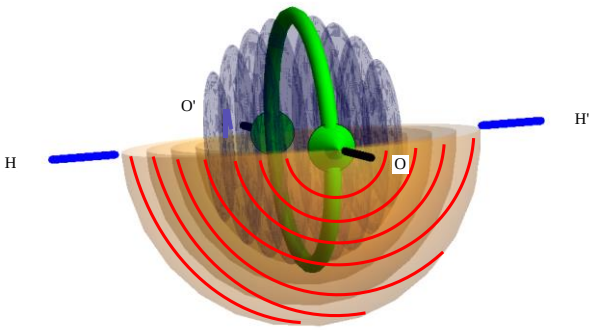

Fig. S6. Schematic of the flat-ellipsoidal droplet structure of the Ch-CNC droplets. The flattened Ch-CNC pseudolayers in the interior (violet) are enclosed by the ellipsoidal peripheral pseudolayers (yellow; only half of the droplet with these pseudolayers is shown). The flattened and ellipsoidal pseudolayers coincide in alignment along the axis HH', but are perpendicular to each other along the ring (shown in green color). Red curves show the director field in one of the Ch-CNC layers that exhibits a defect of strength +1, with the core marked by the green cone; a similar +1 defect forms at the opposite location behind the flattened layers; its core is shown as the green cone at the OO' axis.

Figure S7 shows the TEM image of magnetic Fe_3O_4 NPs that were deposited and dried on the TEM grid.

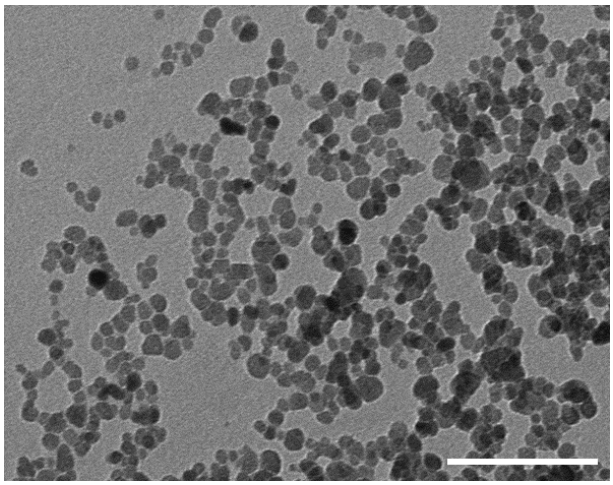

Fig. S7. TEM images of magnetic Fe_3O_4 NPs. The scale bar is 100 nm.

Figure S8 shows low-magnification images of the Ch-CNC droplets laden with magnetic Fe_3O_4 NPs.

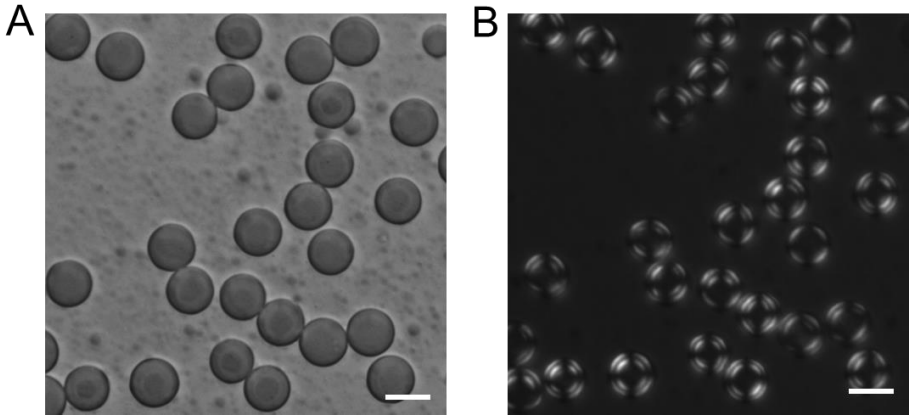

Fig. S8. Characterization of the Ch-CNC droplets loaded with magnetic NPs. Representative bright field (**A**) and POM (**B**) images of the Ch-CNC droplets loaded with Fe_3O_4 NPs ($\phi_{NP} = 1.9\times10^{-3}$). $\phi_0=4.3\times10^{-2}$. The scale bars are 20 μm.

Figure S9 shows a 3D array of the Ch-CNC droplets loaded with magnetic Fe_3O_4 NPs. To recognize the 3D structures of Ch-CNC droplets, we used open circles to illustrate the different layers of droplet packing (fig. S9B). Due to the light scattering of droplets, we could only image two layers of droplets. The droplets in the yellow circles were in the first layer from the top, and the ones in the red circles were in the second layer from the top.

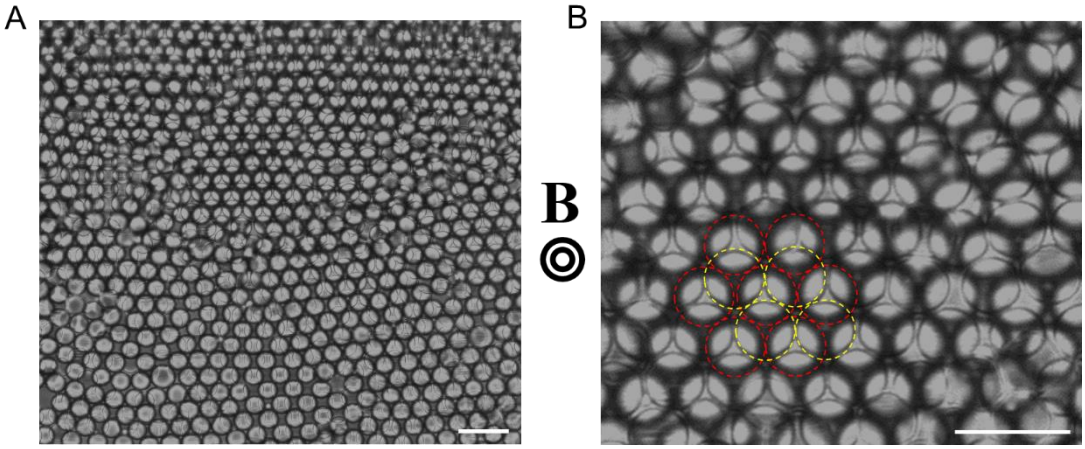

Fig. S9. 3D assemblies of the Ch-CNC droplets loaded with Fe_3O_4 NPs. 3D arrays (**A**) of the Ch-CNC droplets loaded with Fe_3O_4 NPs ($\phi_{NP} = 9.7\times10^{-4}$) under a permanent magnet of 0.35 T. $\phi_0=4.3\times10^{-2}$. The scale bars are 50 μm. (**B**) Enlarged 3D arrays of Ch-CNC droplets shown in (A).

Figure S10 shows low-magnification images of the Ch-CNC droplets loaded with magnetic Fe_3O_4 NPs after the NPs were driven to droplet side facing the magnet (top view).

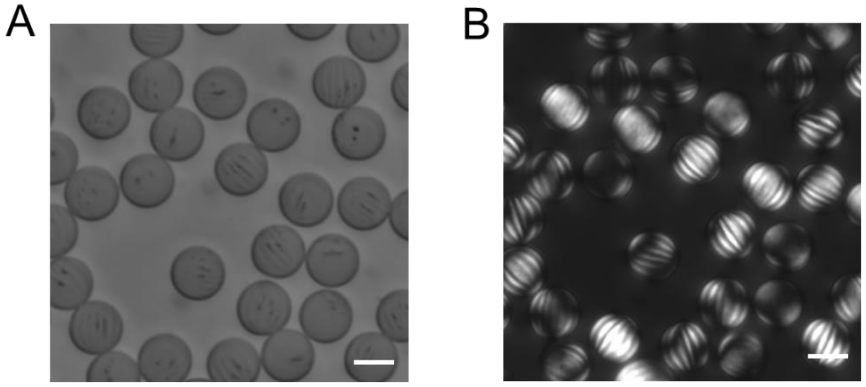

Fig. S10. Characterization of the Ch-CNC droplets with the layers of magnetic NP. Representative bright field (**A**) and POM (**B**) images of the Ch-CNC droplets loaded with Fe_3O_4 NPs at $\phi_{NP} = 9.7\times10^{-4}$, after the NPs were transferred to the droplet side facing the magnet. $\phi_{NP} = 9.7\times10^{-4}$, $\phi_0=4.3\times10^{-2}$ in all the samples. The scale bars are 20 μm.

Figure S11 shows low-magnification images of the dynamic assembly of the Ch-CNC droplets laden with Fe_3O_4 NPs.

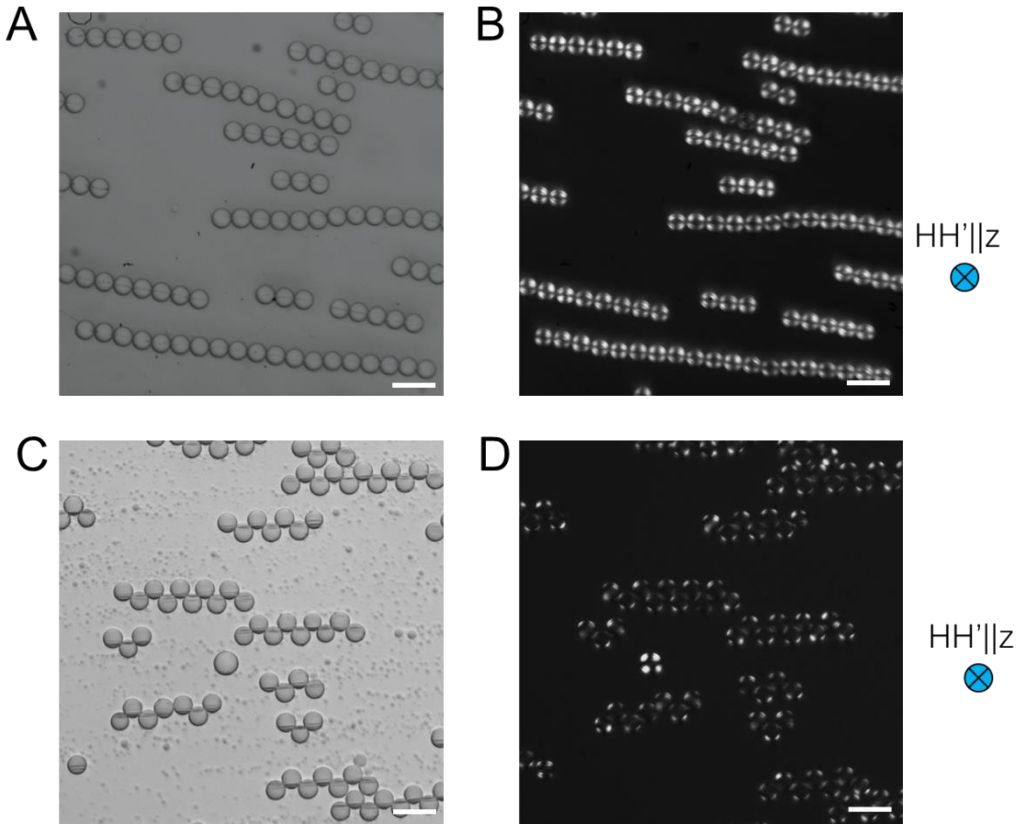

Fig. S11. Two models of assembly of the Ch-CNC droplets laden with Fe_3O_4 NPs under the magnetic field. Bright field (**A**) and POM (**B**) images of the chains formed by the Ch-CNC droplets with BP, TR and CSD assemblies of NPs. Bright field (**C**) and POM (**D**) images of the staggered chains formed by the Ch-CNC droplets loaded with magnetic NPs that were localized in the subsurface layer on one side of the droplets facing the magnet. $\phi_{NP} = 9.7\times10^{-4}$ and $\phi_0=4.3\times10^{-2}$. The scale bars are 50 μm. The HH′ axis was parallel to the z-axis in (B and D).